Progress In Electromagnetics Research M, Vol. 73, 111–118, 2018

Compact Triple-Band Metamaterial Inspired Bandpass Filter with Controllable Transmission Zero Position

Dilip Kumar Choudhary and Raghvendra Kumar Chaudhary*

Abstract—In this paper, a compact triple-band bandpass filter using metamaterial (MTM) inspired structure with controllable transmission zero (TZ) position has been proposed. The gap between feed lines develops electrical coupling and provides series capacitance. An open loop rectangular ring resonator with meander line and rectangular stub develops electric and magnetic couplings separately. Defected ground structure (DGS) provides proper impedance matching and increases the passband. In order to validate metamaterial (MTM) behaviour of designed filter dispersion diagram has been plotted. The position of transmission zero can be controlled by electric and magnetic coupling. The measured operating frequency ranges of three passbands are 1.85–2.15 GHz, 3.55–3.73 GHz and 3.85–4.0 GHz with the 3 dB fractional bandwidth of 15.63, 4.94 and 3.82 percent, respectively. It has minimum insertion loss of 0.7 dB, 0.5 dB and 0.5 dB at the 1st, 2nd, and 3rd passbands, respectively. The electrical size of the proposed filter is $0.16\lambda_g \times 0.15\lambda_g$, where λ_g is the guided wavelength at zeroth order resonance (ZOR) frequency of 1.92 GHz.

1. INTRODUCTION

Increasing demands for wireless services and rapid growth in wireless communication technology urges for compactness and multiband services [1]. It makes multiband filter a very interesting area of research. Further, some triple band bandpass filters have been reported using various concepts [2–6]. A triple band filter using a step-impedance resonator loaded with a stub has been reported [2]. It uses a zero degree feed structure to provide transmission zero (TZ) near passband, which improves bandwidth. In [3], a triple bandpass filter has been designed using multipath resonators and stubs. One passband can be generated due to DGS and other passbands due to stub loaded resonators. A compact triple band bandpass filter has been proposed using a complementary split ring resonator and Koch fractal shape transmission line [4]. In [5], using asymmetric loaded resonators a triple bandpass filter has been designed with wide stopband. To enhance the electromagnetic characteristics of multiband filter multi-mode resonators have been designed in [6]. A multiband filter has also been reported using a stepped impedance resonator and meandered defected ground structure [7] and coplanar waveguide based complementary split ring resonators [8], which provides compactness and design flexibility. To obtain multiband bandpass filter with controllable TZ, separate electric and magnetic couplings (SEMC) with source load coupling has been used [9]. Here SEMC means that electric and magnetic couplings are separated by different paths [10]. Electric coupling path is created by a gap between resonators or metallic patches. Magnetic coupling is formed by via hole or ground shunt (for CPW) or meander line connected with a stub (virtual ground) [11]. The size of above reported work can further be reduced with metamaterial structure.

A revolutionary property of metamaterial (MTM) of effective-homogeneity condition has been utilized to reduce the size of filter [12]. MTMs are artificial engineering electromagnetic structures with

Received 9 July 2018, Accepted 4 September 2018, Scheduled 18 September 2018
* Corresponding author: Raghvendra Kumar Chaudhary (raghvendra.chaudhary@gmail.com).
The authors are with the Department of Electronics Engineering, Indian Institute of Technology (ISM), Dhanbad-826004, India.

negative refractive index and zero phase constant [13]. An MTM filter can be realized using resonant approach and transmission line approach [14]. A tri-band bandpass filter has been reported using a coupled complementary split ring resonator (CSRR) [15]. The transmission line (TL) approach of composite MTM was presented by cascading the series capacitors and shunt inductors with inescapable parasitic series inductance and shunt capacitance [16]. A work has been reported based on composite MTM and parallel step impedance resonator to get a triple passband filter in addition with TZs [17]. In [18], a triple band bandpass filter has been designed using an asymmetric stepped-impedance ring resonator. Two bands are achieved by a stepped-impedance circular ring and third band due to coupling. In [19], a triple band bandpass filter has been proposed with the help of an inverted S-shape resonator, via and rectangular stub. Their frequencies can be controlled by varying the length of the inverted S-shape resonator. Triple band filters have been proposed using a meandered slot defected ground structure and a pair of short-stub/embedded step impedance resonators [20, 21].

Compared with previous works, the proposed filter has the advantages of compact size, minimum insertion loss, and easy fabrication. The transmission zero positions can be controlled by electric and magnetic couplings. The proposed triple-band bandpass filter has been realised with MTM inspired structure using SEMC along source load coupling. Electric coupling is offered by an open loop rectangular ring resonator and a gap between source and load transmission line while magnetic coupling is suggested by a meander line connected through a rectangular stub (virtual ground). The electrical size of the proposed filter is $0.16\lambda_g \times 0.15\lambda_g$ at zeroth order resonance (ZOR) frequency of 1.92 GHz.

2. FILTER DESIGN

2.1. Filter Configuration and Circuit Model

The configuration of the triple band bandpass filter has shown in Fig. 1 with the geometrical parameters in caption. The proposed filter contains an open loop rectangular ring resonator, meaner line, and rectangular stub, gap between input and output ports, and defected ground structure (DGS). A lumped element equivalent circuit diagram of the proposed filter is shown in Fig. 2(a). The gap between source and load provides series left-handed capacitance C_L. The feedline generates series right-handed inductance L_R, and the gap between ports and open loop rectangular resonator provides shunt coupling capacitance C_c. The open loop rectangular resonator generates an inductance L_g and capacitance C_g. The shunt right-handed capacitance C_R is the parasitic capacitance due to substrate. The meander line in shunt will provide shunt left-handed inductance L_L, and rectangular stub which will act as virtual ground will provide shunt capacitance of C_s to ground. DGS provides proper impedance matching. In Fig. 2(b), E and $E1$ represent electric coupling, and M represents magnetic coupling. $R1$ and $R2$ represent rectangular resonators.

2.2. Design Procedure

A flowchart of the design procedure for the proposed triple band filter is illustrated in Fig. 3 and briefly explained with following steps: (i) Assume that the resonance frequencies (f_{01}, f_{02} and f_{03}) of three passbands are 1.9 GHz, 3.7 GHz and 4.0 GHz and return loss (RL) greater than 20 dB and magnetic and electric coupling topology. (ii) Lumped circuit model has been drawn based on coupling topology and metamaterial properties. (iii) Initial lumped element values are calculated using equivalent circuit model along with series and shunt resonance frequencies. (iv) Synthesize the lumped element values ($L_R = 51$ nH, $C_L = 0.55$ pF, $C_c = 0.2$ pF, $L_g = 40$ nH, $C_g = 21$ pF, $C_R = 7.5$ pF, $C_s = 15$ pF, $L_L = 129$ nH) to achieve the desired resonance frequencies, fractional bandwidths, and return loss. (v) Select a Rogers RT/Duroid 6010 substrate (dielectric constant, $\varepsilon_r = 10.2$, loss tangent, $\tan\delta = 0.0023$) with thickness 1.27 mm and input impedance as 50 Ω. (vi) Find the physical layout parameter of the proposed filter based on extracted lumped parameter using well-known formulas of meander line, rectangular ring, stub. (vii) Adjust the physical parameter of the designed filter and compare with desired response.

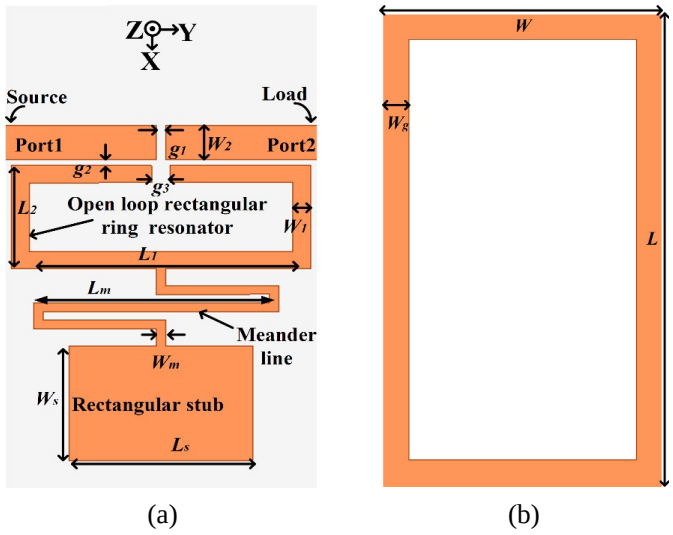

Figure 1. Configuration of proposed filter. (a) Top view. (b) Bottom view [All dimensions are in mm: $L = 17.0$, $W = 10.3$, $L_1 = 8.6$, $W_1 = 0.6$, $L_2 = 3.6$, $W_2 = 1.2$, $L_m = 8$, $W_m = 0.3$, $L_s = 6.0$, $W_s = 4.0$, $g_1 = 0.3$, $g_2 = 0.2$, $g_3 = 0.6$, $W_g = 1.0$].

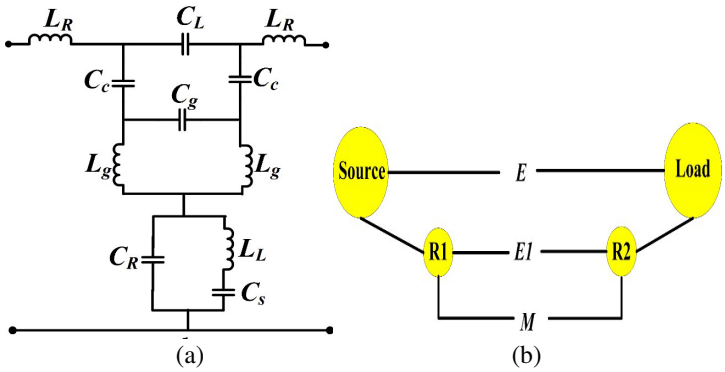

Figure 2. (a) Equivalent circuit diagram of designed filter and (b) coupling topology of proposed filter.

3. RESULTS AND DISCUSSION

In this section, the coupling analysis, comparison between simulated and measured results and parametric analysis have been presented.

3.1. Coupling Analysis

There are six transmission zeros generated due to electric and magnetic couplings of the proposed filter at TZ_1 (1.76 GHz), TZ_2 (2.82 GHz), TZ_3 (3.83 GHz), TZ_4 (4.55 GHz), TZ_5 (4.82 GHz) and TZ_6 (5.12 GHz), respectively. The changes in transmission zero position due to magnetic coupling (because of meander line) are shown in Fig. 4. When the width of meander line (Wm) changes, there is a change in magnetic coupling which causes variation in position of TZ_1 (1.76 GHz). The changes in transmission zero position due to electric coupling (because of gap, g_1, between feedlines) are shown in Fig. 5. As the gap (g_1) between feedlines increases, the electrical coupling decreases which causes increase in position of TZ_2 (2.82 GHz). From Figs. 4 and 5, it is noticed that the changes in position of the fourth, fifth and sixth TZs (namely TZ_4, TZ_5, and TZ_6) are due to combined effect of electric and magnetic couplings.

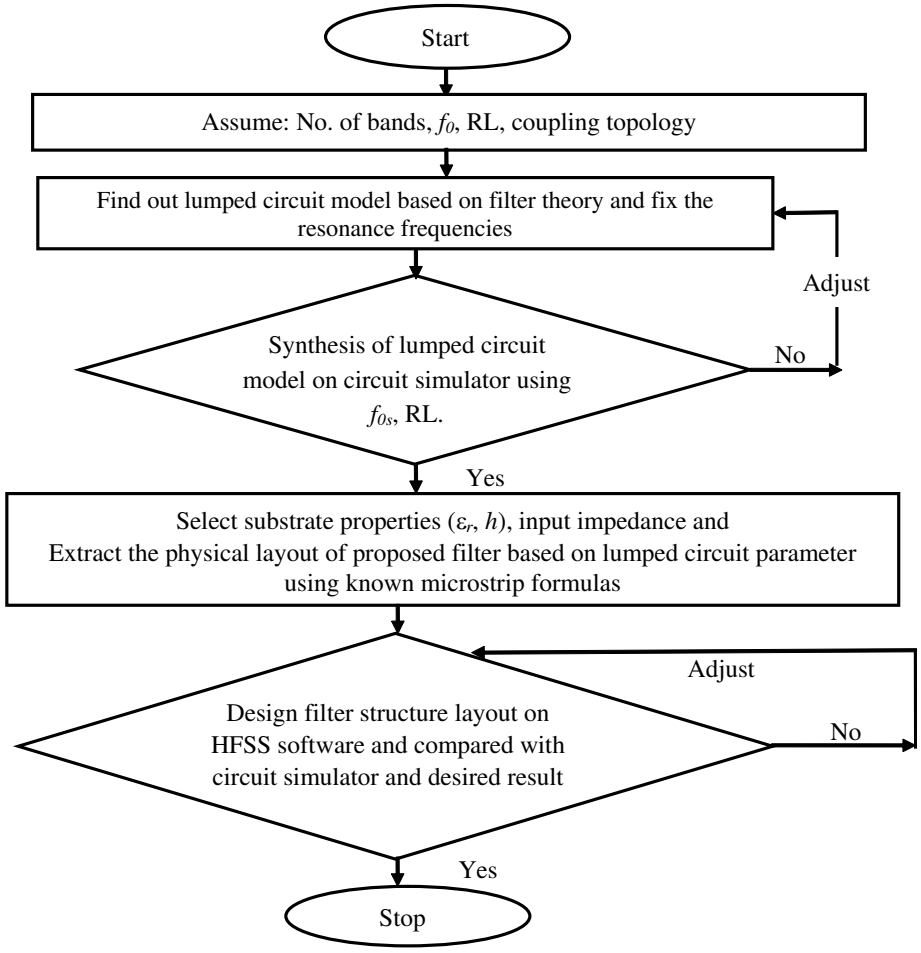

Figure 3. Design procedure of proposed filter using flow chart.

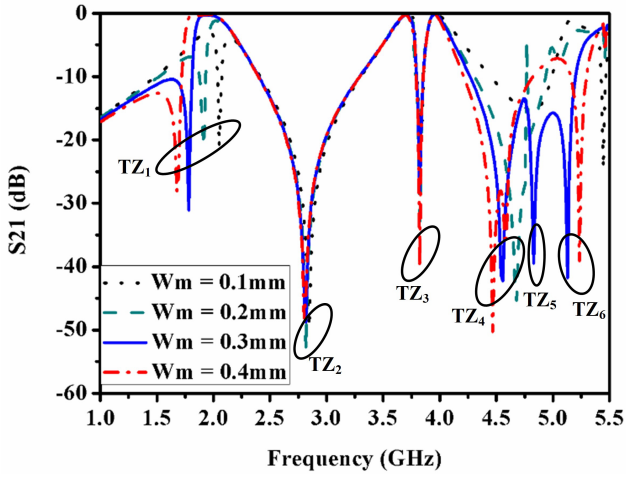

Figure 4. Changes in transmission zero position due to Magnetic coupling (W_m).

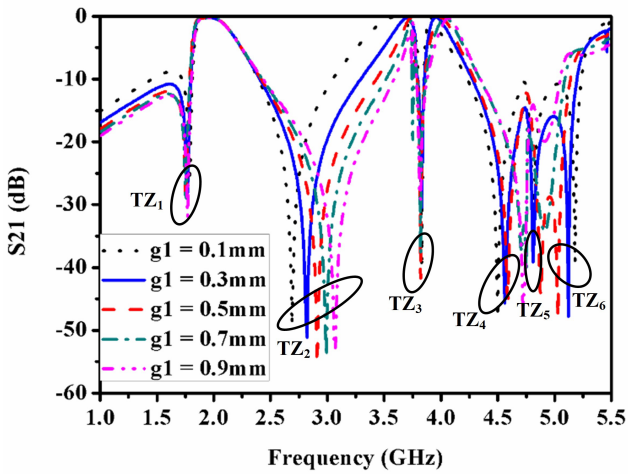

Figure 5. Changes in transmission zero position due to Electric coupling (g_1).

3.2. Simulated and Measured Results

The fabricated prototype of the proposed filter is depicted in Fig. 6. Agilent Vector Network Analyzer N5221A has been used for measurement of scattering parameters. The measured and simulated

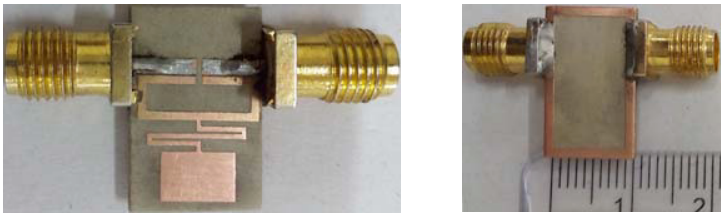

(a) (b)

Figure 6. Fabricated prototype of proposed filter. (a) Top view. (b) Bottom view.

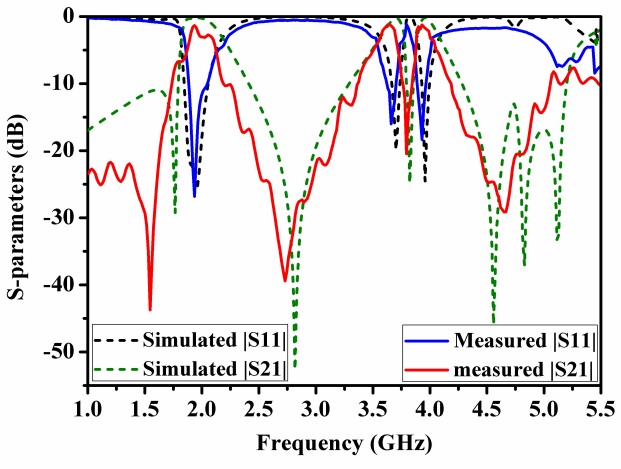

Figure 7. Measured and simulated scattering parameters.

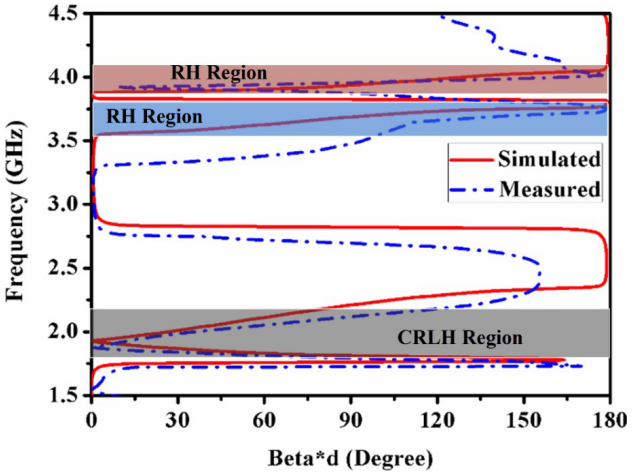

Figure 8. Simulated and measured dispersion diagram.

scattering parameters are presented in Fig. 7. The simulated minimum insertion losses of 0.20 dB (at 1.93 GHz), 0.18 dB (at 3.7 GHz), and 0.1 dB (3.96 GHz) are at the first, second and third passbands, respectively. The return loss is above 20 dB throughout all three passbands. The measured minimum insertion losses are 0.7 dB, 0.5 dB and 0.5 dB at three passbands, respectively. The simulated and measured results are in good agreement, and there is acceptable variation in insertion loss. This variation may be due to imperfection of substrate and connector losses.

The dispersion diagram of designed triple-band bandpass filter using extracted scattering parameters [14] is shown in Fig. 8. It depicts that extension of the first band has both negative and positive slopes, which confirms it as CRLH band from 1.8 GHz to 2.2 GHz. Phase constant becomes zero at 1.92 GHz, known as ZOR frequency. The second band extends from 3.55 GHz to 3.78 GHz with positive slope which validates it as right-handed (RH) band. The third band ranging from 3.85 to 4.1 GHz has a positive slope, known as RH band. A slight shift in measured and simulated dispersion diagrams is due to connector losses.

3.3. Parametric Analysis

The dependency of different resonance frequencies based on electric field distribution is plotted and shown in Fig. 9. It shows that the ZOR frequency 1.93 GHz is influenced by open loop rectangular resonator as well as meander line with a rectangular stub and ground metallic rectangular stub. The second and third passband centre frequencies of 3.7 GHz and 3.96 GHz are affected by electric coupling between feedlines and open loop rectangular resonator.

The dependency of ZOR frequency and resonance frequencies of the 2nd and 3rd passbands based on gap (g_2) between feedline and open loop rectangular ring resonator (OLRRR) and the gap (g_1) between feed lines are shown in Figs. 10(a) and (b), respectively. It is noticed that when 'g_2' increases,

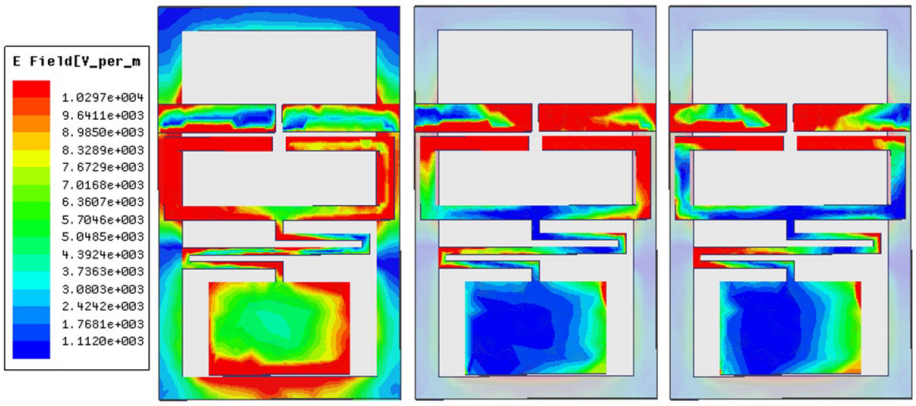

Figure 9. Electric field distribution of triple-band bandpass filter at different frequencies, (a) 1.92 GHz, (b) 3.7 GHz, (c) 3.96 GHz.

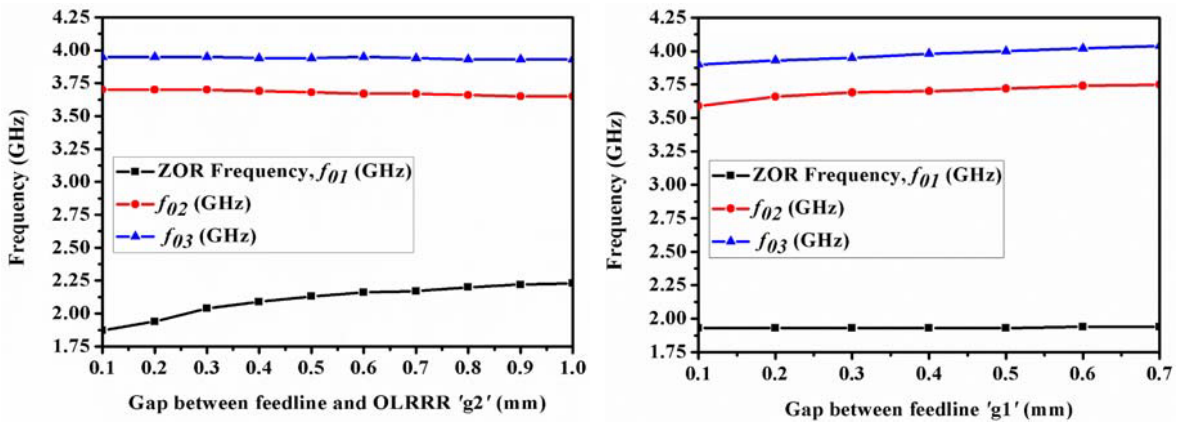

Figure 10. Variation in resonance frequencies with respect to (a) gap 'g_2' between feedline and open loop rectangular ring resonator, and (b) gap 'g_1' between feedline.

the value of electrical coupling capacitance, Cc, which causes the increase of the ZOR frequency towards higher value. The 2nd and 3rd passband resonance frequencies remain constant when g_2 varies. The variation in the 2nd and 3rd passband resonance frequencies is mainly due to the gap (g_1) between feed line. Hence the ZOR frequency varies mainly due to coupling capacitance C_c. To justify the proposed structure, comparison of performance has been made among earlier published triple-band

Table 1. Comparison of designed filter with earlier published triple band bandpass filter.

	This work	**[2]**	**[5]**	**[6]**	**[16]**
Centre frequencies (GHz)	**1.92/3.65/3.92**	1.93/3.6/4.89	1.37/2.43/3.53	1.95/3.5/5.2	2.1/5/7/7.3
FBW (%)	**15.6/4.9/3.8**	19.2/11.6/2.86	4.4/5.9/2.7	8.5/3.7/3.9	57.1/8.7/4.1
Insertion loss (dB)	**0.7/0.5/0.5**	-	1.7/1.8/2.5	0.46/1.96/1.15	0.8/1.6/2.4
Return loss (dB)	**27/16/18.5**	15/15/22	18/21/20	>16.7	25.5/15/23
Number of TZs	**6**	7	3	3	4
Size ($\lambda_g \times \lambda_g$)	**0.16 × 0.15**	0.33 × 0.23	0.26 × 0.13	0.38 × 0.28	0.23 × 0.21

bandpass filters and the proposed one, as shown in Table 1. This table shows that the proposed filter has advantages of low insertion loss, good 3 dB fractional bandwidth (FBW) and compact size. The proposed filter has electrical size of $0.16\lambda_g \times 0.15\lambda_g$ at ZOR frequency 1.92 GHz, where λ_g is guided wavelength.

4. CONCLUSION

A compact triple-band bandpass metamaterial filter with controllable transmission zero position has been proposed. The filter TZs position depends on SEMC and mixed coupling of structure. The defected ground structure increases the passband of designed filter. The proposed filter is in good agreement with simulated and measured results. The proposed filter has three passbands of 1.85–2.15 GHz, 3.55–3.73 GHz and 3.85–4.0 GHz. The measured insertion losses within these passbands are 0.7 dB, 0.5 dB and 0.5 dB. The return losses are 27 dB, 16 dB and 18.5 dB at center frequencies of proposed passbands, respectively. The proposed filter has compact electrical size of $0.16\lambda_g \times 0.15\lambda_g$, at ZOR frequency. The advantage of filter is compact size and good selectivity due to higher number of transmission zeros, useful for triple band wireless communication.

REFERENCES

1. Xu, J., W. Wu, and G. Wei, "Compact multi-band bandpass filters with mixed electric and magnetic coupling using multiple-mode resonator," *IEEE Transactions on Microwave Theory and Techniques*, Vol. 63, 3909–3919, 2015.
2. Kumar, N. and Y. K. Singh, "Compact Tri-band bandpass filter using three stub-loaded open loop resonator with wide stopband and improved bandwidth response," *Electronics Letters*, Vol. 50, 1950–1952, 2014.
3. Wu, H. W., L. Y. Jian, Y. W. Chen, and Y. K. Su, "New triple passband bandpass filter using multipath stub loaded resonators," *IEEE Microwave and Wireless Components Letters*, Vol. 26, 186–188, 2016.
4. Xu, H. X., G. M. Wang, and J. G. Liang, "Novel designed CSRRs and its application in tunable tri-band bandpass filter based on fractal geometry," *Radioengineering*, Vol. 20, 312–316, 2011.
5. Lan, S., M. Weng, S. Chang, C. Hung, and S. Liu, "A tri-band bandpass filter with wide stopband using asymmetric stub-loaded resonators," *IEEE Microwave and Wireless Components Letters*, Vol. 25, 19–21, 2015.
6. Fan, W. X., Z. P. Li, and S. X. Gong, "Tri-band filter using combined E-type resonators," *Electronics Letters*, Vol. 49, 193–194, 2013.
7. Koirala, G. R. and N. Y. Kim, "Multiband bandstop filter using an I-stub-loaded meandered defected microstrip structure," *Radioengineering*, Vol. 25, 61–66, 2016.
8. Choudhary, D. K. and R. K. Chaudhary, "A compact CPW-based dual-band filter using modified complementary split ring resonator," *International Journal of Electronics and Communications (AEU)*, Vol. 89, 110–115, 2018.
9. Xiao, J. K., Y. Li, J. G. Ma, and X. P. Bai, "Transmission zero controllable bandpass filters with dual and quad-band," *Electronics Letters*, Vol. 51, 1003–1005, 2015.
10. Ma, K., J. G. Ma, K. S. Yeo, and A. M. Do, "A compact size coupling controllable filter with separate electric and magnetic coupling paths," *IEEE Transactions on Microwave Theory and Techniques*, Vol. 54, 1113–1119, 2006.
11. Xiao, J. K., M. Zhu, Y. Li, and J. G. Ma, "Coplanar waveguide bandpass filters with separate electric and magnetic couplings," *Electronics Letters*, Vol. 52, 122–124, 2016.
12. Caloz, C. and T. Itoh, *Electromagnetic Metamaterials: Transmission Line Approach and Microwave Applications*, Wiley, Hoboken, NJ, USA, 2006.
13. Choudhary, D. K. and R. K. Chaudhary, "A compact coplanar waveguide (CPW)-fed zeroth-order resonant filter for bandpass applications," *Frequenz Journal of RF-Engineering and Telecommunications, De Gruyter*, Vol. 71, 305–310, 2017.

14. Choudhary, D. K. and R. K. Chaudhary, "Vialess wideband bandpass filter using CRLH transmission line with semi-circular stub," *International Conference on Microwave and Photonics (ICMAP)*, 1–2, Dhanbad, India, 2015.
15. Wei, F., P. Y. Qin, Y. J. Guo, C. Ding, and X. W. Shi, "Compact balanced dual and tri-band BPFs based on coupled complementary split ring resonators (C-CSRR)," *IEEE Microwave and Wireless Components Letters*, Vol. 26, 107–109, 2016.
16. Kumar, A., D. K. Choudhary, and R. K. Chaudhary, "Metamaterial tri-band bandpass filter using meander-line with rectangular-stub," *Progress In Electromagnetics Research Letters*, Vol. 66, 121–126, 2017.
17. Cao, H., M. Yi, H. Chen, J. Liang, Y. Yu, X. Tan, and S. Yang, "A novel compact tri-band bandpass filter based on dual-mode CRLH-TL resonator and transversal stepped-impedance resonator," *Progress In Electromagnetics Research Letters*, Vol. 56, 53–58, 2015.
18. Wang, W., Y. Li, Q. Cao, S. Yang, and Y. Chen, "Design of triple-bandpass filters using an asymmetric stepped-impedance ring resonator," *Progress In Electromagnetics Research Letters*, Vol. 67, 7–12, 2017.
19. Choudhary, D. K. ands R. K. Chaudhary, "A compact triple band metamaterial inspired bandpass filter using inverted S-shape resonator," *Radioengineering*, Vol. 27, 373–378, 2018.
20. Ning, H., J. Wang, Q. Xiong, and L. Mao, "Design of planar dual and triple narrow-band bandstop filters with independently controlled stopbands and improved spurious response," *Progress In Electromagnetics Research*, Vol. 131, 259–274, 2012.
21. Xu, K., Y.-H. Zhang, D. Li, Y. Fan, J. L.-W. Li, W. T. Joines, and Q. H. Liu, "Novel design of a compact triple-band bandpass filter using short stub-loaded SIRs and embedded SIRs structure," *Progress In Electromagnetics Research*, Vol. 142, 309–320, 2013.